Top Catal (2013) 56:1922–1936
DOI 10.1007/s11244-013-0129-8

ORIGINAL PAPER

Cyclic Lean Reduction of NO by CO in Excess H_2O on Pt–Rh/Ba/Al_2O_3: Elucidating Mechanistic Features and Catalyst Performance

Prasanna Dasari · Rachel Muncrief · Michael P. Harold

Published online: 4 July 2013

Abstract This study provides insight into the mechanistic and performance features of the cyclic reduction of NO_x by CO in the presence and absence of excess water on a Pt–Rh/Ba/Al_2O_3 NO_x storage and reduction catalyst. At low temperatures (150–200 °C), CO is ineffective in reducing NO_x due to self-inhibition while at temperatures exceeding 200 °C, CO effectively reduces NO_x to main product N_2 (selectivity >70 %) and byproduct N_2O. The addition of H_2O at these temperatures has a significant promoting effect on NO_x conversion while leading to a slight drop in the CO conversion, indicating a more efficient and selective lean reduction process. The appearance of NH_3 as a product is attributed either to isocyanate (NCO) hydrolysis and/or reduction of NO_x by H_2 formed by the water gas shift chemistry. After the switch from the rich to lean phase, second maxima are observed in the N_2O and CO_2 concentrations versus time, in addition to the maxima observed during the rich phase. These and other product evolution trends provide evidence for the involvement of NCOs as important intermediates, formed during the CO reduction of NO on the precious metal components, followed by their spillover to the storage component. The reversible storage of the NCOs on the Al_2O_3 and BaO and their reactivity appears to be an important pathway during cyclic operation on Pt–Rh/Ba/Al_2O_3 catalyst. In the absence of water the NCOs are not completely reacted away during the rich phase, which leads to their reaction with NO and O_2 upon switching to the subsequent lean phase, as evidenced by the evolution of N_2, N_2O and CO_2. In contrast, negligible product evolution is observed during the lean phase in the presence of water. This is consistent with a rapid hydrolysis of NCOs to NH_3, which results in a deeper regeneration of the catalyst due in part to the reaction of the NH_3 with stored NO_x. The data reveal more efficient utilization of CO for reducing NO_x in the presence of water which further underscores the NCO mechanism. Phenomenological pathways based on the data are proposed that describes the cyclic reduction of NO_x by CO under dry and wet conditions.

Keywords NO_x · CO · Platinum · Barium · Lean NO_x trap · Isocyanates

P. Dasari · R. Muncrief · M. P. Harold (✉)
Department of Chemical & Biomolecular Engineering, University of Houston, Houston, TX 77204-4004, USA
e-mail: mharold@uh.edu

1 Introduction

Diesel and lean burn gasoline engines are gaining increased attention lately owing to their higher fuel efficiency and lower CO_2 emissions than stoichiometric engines. However, they are a major source of NO_x emissions and as a result are subject to increasingly stringent emission standards worldwide, notably in Europe (emerging Euro 6 rules) and the USA. Unfortunately, the three way catalyst emission aftertreatment technology used for stoichiometric gasoline engines is ineffective in reducing NO_x in the presence of excess O_2. This scenario has led to an extensive research in the development of lean NO_x reduction technologies, including Selective Catalytic Reduction (SCR) of NO_x and NO_x storage reduction (NSR).

Ammonia-based SCR is an effective lean NO_x reduction technology employing Fe- and Cu-exchanged zeolite and vanadia catalysts [1, 2]. SCR is primarily suited for heavy-duty vehicles and engines since the fixed cost of the aqueous urea feed system is too high for light-duty applications [3]. In contrast, NSR, carried out in the Lean NO_x trap (LNT) is

suitable for light-duty diesel engines. Typical LNT catalysts consist of a high surface area support (γ-Al_2O_3), precious metals (Pt, Rh) and a storage component (alkali/alkaline earth metal oxides like BaO). The LNT is operated with lean-rich cycling; NO_x is stored on the storage component during the longer lean phase and the trapped NO_x is then reduced on the precious metals by reductants like CO, H_2 and HC's during the abbreviated rich phase. The main N-containing products are N_2 (desired) and byproducts NH_3 and N_2O. Emerging in some applications is the combined LNT/SCR technology in which NH_3 is generated in situ during the LNT regeneration and is consumed through reaction with NO_x in the downstream SCR. Whether a stand-alone LNT or one combined with SCR, NH_3 is a critical species whose formation, reaction mechanism and kinetics must be fully understood to develop optimal LNT design and operating strategies.

A large number of studies have investigated the mechanisms, kinetics and catalyst performance features of NO_x storage [4–9] and reduction [10–13]. A review captures more recent developments [14]. The NO_x reduction chemistry using H_2 as the reductant is by now well established; among other features, ammonia is a major intermediate during the catalytic regeneration of stored nitrates by H_2 under isothermal conditions [11, 13, 15]. A H_2 front moves down the monolith length as nitrates/nitrites are regenerated by a two-step reaction mechanism, generating NH_3 first, which then reacts further with stored NO_x species and adsorbed oxygen to make N_2. Progress has been made in understanding the behavior of other reductants like CO and hydrocarbons [16–18], but more work is needed to unravel the complex chemistry characterized by coupled reaction chemistry and transport effects. When using CO as a reductant, NH_3 is formed in addition to N_2 and N_2O without any H other than that in H_2O being fed to the catalyst [19]. In such a case two major routes to NH_3 formation are possible. The first is by the water–gas shift (WGS) reaction of CO and H_2O to give CO_2 and H_2, the latter of which then reacts with NO to give NH_3. A second pathway is through reaction between NO and CO forming surface isocyanates (–N=C=O)/cyanates (N≡C–O–) [20], which are readily hydrolyzed to form NH_3 in the presence of water. The contribution of both the pathways is of significance because each proceeds in the presence of high exhaust concentration of H_2O (5–15 %).

Table 1 summarizes a few surface IR measurements that have shown the existence of isocyanate and cyanate species formation during the reduction of NO by CO on precious metals both unsupported and supported on various oxides including alumina and silica. Unland [20] first reported the formation of isocyanate species during the interaction of NO and CO on Pt/Al_2O_3 through infrared spectra of species adsorbed on the catalyst. Solymosi and co-workers [21–25, 29] studied the formation and stability of isocyanates during the reaction of NO and CO on various precious metals (Pt, Pd, Rh), both unsupported and supported on various oxides. They showed through infrared studies that NCO species are formed on the precious metals through the reaction of gas phase CO and adsorbed N formed in the dissociation of adsorbed NO, and that these isocyanates are highly unstable on precious metals, readily dissociating to adsorbed N and CO. On supported catalysts (Al_2O_3, SiO_2), the migration of NCO from the precious metal onto the support is a very fast process. Moreover, these isocyanates are thermally stable on the support under dry conditions. Miners et al. [30] studied the NO + CO reaction on Pt(100) using in situ infrared absorption spectroscopy (IRAS) and observed isocyanate formation over a narrow temperature range of 380–400 K. They proposed that NCO formation becomes favorable once the concentration of N atoms on the surface is low and, more importantly, when the diffusion of these atoms becomes severely hindered by the high coverage of CO. They further suggested that the dissociation of NCO species requires vacant sites. Miyadera and co-workers [27, 28] studied the formation of NCO and its reactivity with NO, O_2 and NO + O_2 mixtures on Ag/Al_2O_3 by a pulse reaction technique and an in situ diffuse reflectance infrared Fourier transform spectroscopy. Forzatti and co-workers [31, 32] studied the reduction of previously stored NO_x by CO on Pt–Ba/Al_2O_3 both in the presence and absence of water by means of transient response methods. They proposed a two-step reaction scheme wherein the stored nitrates are reduced to nitrites and surface isocyanate/cyanate species; these species further react with residual nitrites to give N_2. In the presence of H_2O the isocyanates are readily hydrolyzed to ammonia. They will also react with O_2 and/or NO, NO_2 to give N_2, N_2O and CO_2 [33–37]. Burch and co-workers [38, 39] studied the reduction of NO_x by CO and H_2 on Ag/Al_2O_3 catalyst and showed that two types of isocyantes species are formed on the oxide support; an active isocyanate species close to the metal crystallite—support interface, and a spectator isocyanate species far from the interface, especially during prolonged exposure to the reductant CO. Their study suggests that while a high surface concentration of isocyanates may be measured, this does not imply that all of these species are active intermediates during the reduction of NO_x by CO. Rather, the isocyanate spectators may in fact reduce the overall NO_x storage capacity of the catalyst. Recently a few research groups [31, 32, 40–43] studied the reduction of stored NO_x by CO over Pt–BaO/Al_2O_3 and Pt–K/Al_2O_3 catalysts and suggested that cyanate/isocyanate ad-species could act as a precursor to N_2 formation as they can reduce the stored nitrates/nitrites. They also suggested that rate of isocyanate formation is faster than the rate of reaction between the

isocyanates and stored nitrates/nitrites. These studies involved the pre-storage of NO_x up to saturation followed by prolonged exposure to reductant (1–10 min). This procedure is not typical of conventional NSR operation and may lead to significant accumulation of isocyanates, complicating the interpretation of their reactivity.

In our recent study [19], differential steady-state kinetics experiments revealed the existence of CO inhibition for the CO + NO, CO + H_2O, and CO + NO + H_2O systems which was more significant in the absence of H_2O. We showed that the NH_3 formation in the CO + NO + H_2O system was consistent with the coupled NO + CO and WGS (CO + $H_2O \rightarrow H_2 + CO_2$) chemistries under anaerobic conditions. The data showed that CO adsorption/inhibition was more pronounced for the NO + CO reaction (reaction order is −1) than for the WGS reaction (reaction order is −0.23). The results suggest that during the steady state anaerobic reduction of NO by CO in the presence of water, NH_3 is mainly produced by the reduction of NO by surface hydrogen formed as an intermediate during the WGS reaction and CO scavenges surface O to form CO_2. Contribution by the isocyanate hydrolysis pathway appeared to be secondary under steady state conditions.

Here we extend the study to transient lean storage and reduction of NO_x. The transient operation simulates typical NSR operation involving the fast lean–rich cycling conditions in which the storage lasts for about a minute and the regeneration for only a few seconds. The effects of temperature and feed composition are studied through a detailed investigation of the transient NO_x and reductant conversion and product distribution trends. The roles of H_2O and CO_2 are studied, as they are the major components of actual exhaust. The transient experiments show convincing evidence of an isocyanate route involving the support/storage phase (Al_2O_3/BaO). The effects of various operating conditions like catalyst temperature and feed composition on the yield of NH_3 provide further insight about the cyclic operation with CO as the reductant. Finally, a phenomenological mechanism is presented that builds on the current understanding of the cyclic reduction of NO_x by CO under dry and wet conditions.

2 Experimental

2.1 Catalyst

The catalyst samples used for these experiments were monolith catalysts provided by BASF (Iselin, New Jersey). Larger cylindrical cores (D = 3.8 cm and L = 7.6 cm) were cut using a dry diamond saw to a smaller, nearly cylindrical shape (88 channels; D = 1.3 cm, L = 3.0 cm). The washcoat contained 1.13 % PGM (Pt, Rh), 24.5 % BaO, and remainder γ-alumina with an overall mass loading of 4.6 g/in.^{3} monolith. The washcoat was supported on a cordierite structure (62 channels/cm^2). The sample was wrapped in Fiberfrax® ceramic paper that had been pretreated and then placed in a quartz tube flow reactor. The catalyst was not exposed to temperatures exceeding ca. 500 °C to avoid sintering and subsequent loss in activity.

2.2 Flow Reactor Set-Up

The experimental set-up used in this study is similar to the one used in previous studies [19] and comprised four major

Table 1 Surface measurements of isocyanate formation on precious metal based catalysts

Research group	Catalyst	Reaction conditions at which surface isocyanates were measured	Measurement techniques employed
Unland [20]	Pt/Al_2O_3	T ≥ 300 °C, NO + CO	Infrared spectroscopy
Rasko and co-workers [21–23, 25]	Pt, Pt/Al_2O_3 and Ir/Al_2O_3	T(150 °C), NO + CO	Infrared spectroscopy
Solymosi et al. [24]	Pt supported on SiO_2, MgO, Al_2O_3, and MgO	T(250, 400 °C), NO + CO	Infrared spectroscopy
Hecker et al. [26]	Rh/SiO_2	T(225 °C), NO + CO	Infrared spectroscopy
Miyadera and co-workers [27, 28]	Al_2O_3, Ag/Al_2O_3	T ≥ 150 °C, NO + O_2 + C_2H_5OH	Infrared spectroscopy
Miners et al. [30]	Pt(100)	T(107–127 °C), NO + CO	in situ vibrational spectroscopy (IRAS)
Forzatti et al. [31]	$Pt–Ba/Al_2O_3$	T(350 °C), lean-rich cycling of NO + O_2 and CO	FT-IR analysis
Burch and co-workers [38, 39]	Ag/Al_2O_3	T(245 °C), NO_x + Octane + H_2	Short time-on-stream in situ spectroscopic transient isotope experimental techniques (STOS-SSITKA)

components: a feed system, a reactor system, an analytical system, and a data acquisition system. A bank of gas cylinders (Praxair) and mass flow controllers (MKS Inc.) were utilized to simulate the feed gas mixtures. A syringe pump (Teledyne Isco model 100DX) was used for injecting water into the reactor system. In order to achieve a constant feed rate of water, a needle valve was used to reduce the pressure while at high temperature, causing flash vaporization. Stainless steel tubing of 1/16 in. diameter was used to introduce the water vapor directly into the carrier gas stream by way of a bored-through fitting. The reactor system consisted of a quartz tube flow reactor positioned inside a Thermocraft™ tube furnace. The reactor temperature was monitored with three K-type stainless steel sheathed thermocouples (OD = 0.75 mm). One thermocouple measured the catalyst temperature (T_c) which was positioned within an internal monolith channel at the approximate mid-point of the monolith (radial and axial) while the gas feed (T_f) and outlet (T_o) temperatures were monitored by thermocouples positioned 1 cm upstream of the catalyst and the other 0.2 cm downstream of the catalyst, respectively.

All the gas lines were heated and maintained at 140 °C to prevent water condensation and to minimize adsorption of NH_3. The total gas flow rate was 3 L/min, corresponding to a gas hourly space velocity of 42,000 h^{-1}. The outlet NO, NO_2, N_2O, NH_3, H_2O, CO and CO_2 concentrations were monitored by a FTIR spectrometer (Thermo Scientific, 6700 Nicolet). Analog signals from the thermocouples, pressure gauge and mass flow controllers were sent to a National Instruments module to digitize the signals. These data were recorded on a PC using Labview® Software while the FT-IR composition data was collected on another PC using OMNIC Software. In order to synchronize the outputs from FTIR analyzer and the Labview Software, tracer studies were carried out to determine the time delays and a lag of 6 s was accounted for. An overall N material balance enabled an estimate of the N_2 selectivity.

2.3 Lean and Rich Cycling Experiments

Several integral experiments of three reduction phase mixtures were carried out over the temperature range of 150–400 °C: (i) CO; (ii) CO + H_2O; and (iii) CO + H_2O + CO_2. Mass flow controllers were used to control the lean and rich phase concentrations. For the cycling experiments, the storage step comprised a feed containing 500 ppm NO and 4 % O_2 in Ar (60 s), while the rich pulse contained varying concentrations of the reductant in Ar (10 s). For the experiments involving H_2O and CO_2, 5 % H_2O and 3 % CO_2 was added during the entire lean-rich cycle. The cycle-averaged results were obtained over at least 9 cycles after the system had reached a transient steady state. To reach a transient steady state, it took approximately 10–30 cycles depending on the conditions but minimally 40 cycles were run at each experimental condition. The total NO_x stored (mol) per lean step was calculated by

$$\mathrm{NO_x^{stored}}(t_s) = \int_0^{t_S} [F^{\mathrm{o}}_{\mathrm{NO}} - F_{\mathrm{NOx}}(t)]dt \quad (1)$$

where s denotes storage, t_s is the storage time (s), $F^{\mathrm{o}}_{\mathrm{NO}}$ (mol/s) is the feed rate of NO and $F_{\mathrm{NO_x}}$ (mol/s) is the sum of the effluent molar flow rates of NO and NO_2. The cycle-averaged NO_x conversion was calculated by

$$X_{\mathrm{NO_x}} = \frac{\int_0^{t_{S+R}} [F^{\mathrm{o}}_{\mathrm{NO}}(t) - F_{\mathrm{NOx}}(t)]dt}{\int_0^{t_{S+R}} F^{\mathrm{o}}_{\mathrm{NO}}(t)dt} \quad (2)$$

where t_{s+R} is the total cycle time (s). The corresponding product selectivities to NH_3 and N_2O for the entire cycle are defined as

$$S_{\mathrm{NH_3}} = \frac{100 \times \int_0^{t_{S+R}} F_{\mathrm{NH_3}}(t)dt}{\int_0^{t_{S+R}} [F^{\mathrm{o}}_{\mathrm{NO}}(t) - F_{\mathrm{NOx}}(t)]dt} \quad (3)$$

$$S_{\mathrm{N_2O}} = \frac{2 \times 100 \times \int_0^{t_{S+R}} F_{\mathrm{N_2O}}(t)dt}{\int_0^{t_{S+R}} [F^{\mathrm{o}}_{\mathrm{NO}}(t) - F_{\mathrm{NOx}}(t)]dt} \quad (4)$$

where $F_{\mathrm{NH_3}}$ and $F_{\mathrm{N_2O}}$ (mol/s) are the effluent molar flow rates of NH_3 and N_2O respectively. Since the concentration of N_2 is not measured the product selectivity to N_2 is defined as

$$S_{\mathrm{N_2}} = 100 - S_{\mathrm{NH_3}} - S_{\mathrm{N_2O}} \quad (5)$$

3 Results and Discussion

3.1 Cyclic Reduction of NO by CO in the Absence of Water

The baseline catalyst performance was examined by conducting NO/O_2 + CO cycling studies in the absence of H_2O over a wide range of feed temperatures and CO feed concentrations. Cycle-averaged conversion and selectivity data in the absence of H_2O will be reviewed first followed by a closer examination of representative instantaneous transient data. The lean phase comprised a mixture of 500 ppm NO and 4 % O_2 with balance Ar for 60 s. The rich phase contained CO (in Ar) with CO feed concentration varied from 0.5 % (5,000 ppm) to 2.5 % (25,000 ppm) in 0.5 % increments.

Figure 1 shows the temperature dependence of the cycle-averaged conversion of NO_x (a) and CO (b) and the product selectivity to N_2O (c) and N_2 (d) for four CO feed concentrations. The NO_x conversion increased sharply between 200 and 250 °C, from level <10 % to a constant level that increased with the CO concentration. The CO

conversion was nearly complete for temperatures exceeding 300 °C and CO concentrations <1.5 %, indicating reductant-limited conditions. Complete NO_x conversion was obtained for 2 % CO and T ≥ 300 °C. The N_2O selectivity exhibited a local maximum at 200 °C and, with N_2 being the only other product, its selectivity had a local minimum at the same temperature. The product distribution was sensitive to temperature even in the range for which the NO_x conversion was constant. For example, the N_2 (N_2O) selectivity sharply increased (decreased) with temperature between 200 and 400 °C. The selectivity was essentially independent of the CO feed concentration at higher temperatures, while the selectivities were quite sensitive to the CO concentration at low temperatures (T < 250 °C).

To examine the CO effect in more detail, a series of cycling experiments was carried out by varying the CO feed concentration during the rich pulse while keeping the feed temperature and lean phase composition constant. Figure 2 shows the cycle-averaged conversions of NO_x and CO (a, b) and product selectivities to N_2O and N_2 (c, d) as a function of the CO feed concentration for temperatures in the 150–300 °C range. The T ≤ 200 °C conversion data show very low NO_x conversion (<10 %) but somewhat higher CO conversions. For T ≥ 250 °C the NO_x and CO conversions were significantly higher. The decreasing (increasing) dependence of CO (NO_x) conversion with CO concentration reflects the shift from reductant to NO_x limited conditions. At 300 °C complete conversion of CO was obtained at the lower feed CO concentrations (≤10,000 ppm) whereas nearly complete conversion of NO_x was obtained at 20,000 ppm of CO. The N_2O and N_2 selectivities moderately decreased and increased with CO concentration, respectively (Fig. 2c, d) with the highest N_2 selectivity (~82 %) achieved at 300 °C over the entire CO concentration range.

The transient dependencies of the measured products CO_2 and N_2O help to explain the trends in the cycle-averaged conversions and selectivities. Specific features of the temporal profiles of N_2O and CO_2 infer a rather complex reaction system. Before analyzing the data in detail it is instructive to present the following set of adsorption, desorption, and reaction steps. (We use the numbering system of our steady-state study [19]. Stable reactants and products are shown in *bold*.) The main reacting species adsorb and desorb on the precious metal sites (*):

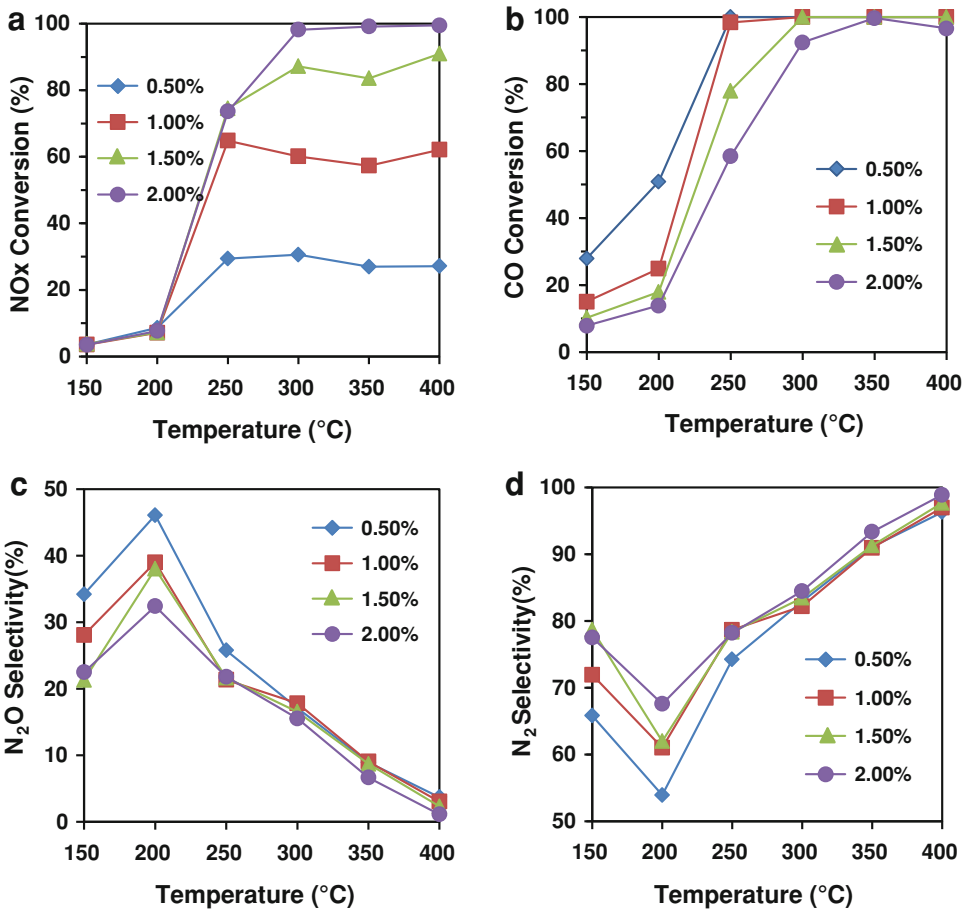

Fig. 1 Conversion of **a** NO_x and **b** CO and product selectivity to **c** N_2O and **d** N_2 as a function of reaction temperature during the cyclic reduction of NO by CO at various feed concentrations of CO during the rich phase (*Lean*: 500 ppm NO + 4 % O_2, 60 s; *Rich* 0.5–2.0 % CO, 10 s; balance: Ar); *Total flowrate* 3,000 sccm

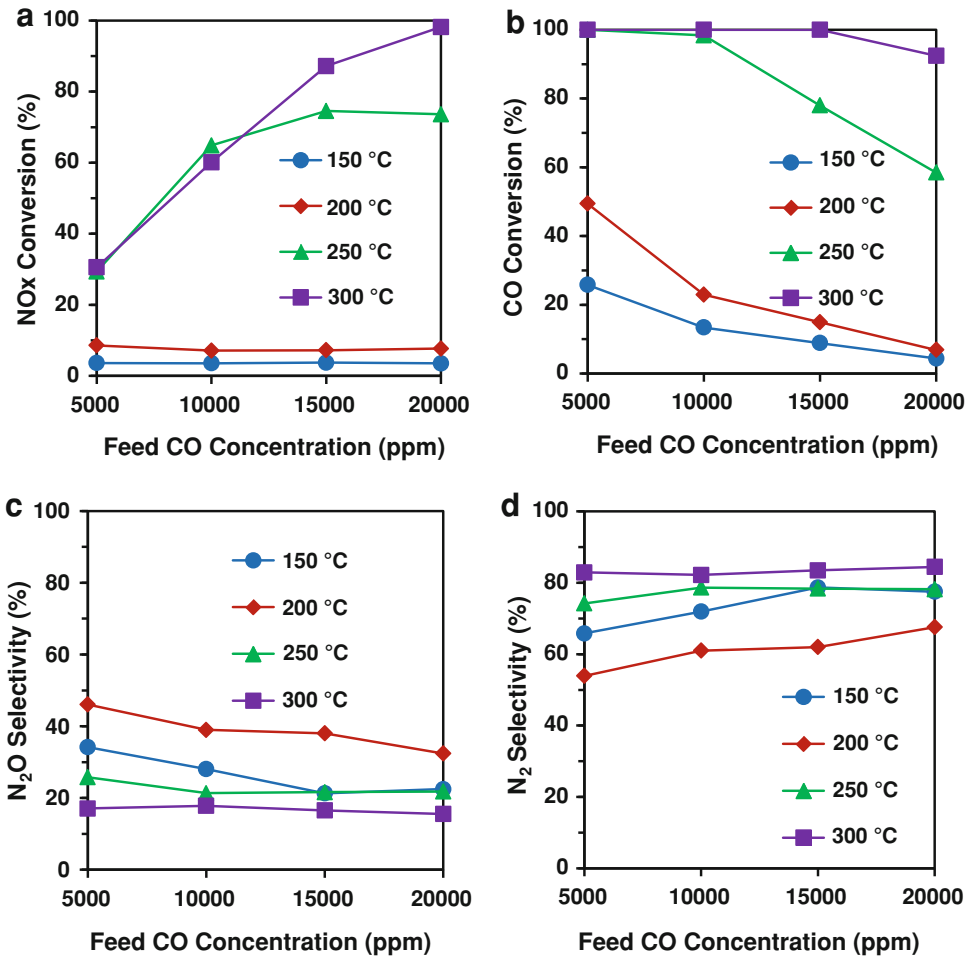

Fig. 2 Reactant conversion of **a** NO_x, **b** CO and product distribution of **c** N_2O and **d** N_2 as a function of the feed concentration of CO during the cyclic reduction of NO_x by CO at 150, 200, 250 and 300 °C (*Lean* 500 ppm NO + 4 % O_2, 60 s; *Rich* 5,000–20,000 ppm of CO, 10 s; *balance* Ar); *Total flowrate* 3,000 sccm

$$\text{S1}: \mathbf{NO} + {}^* \longleftrightarrow \text{NO}^*$$
$$\text{S2}: \mathbf{CO} + {}^* \longleftrightarrow \text{CO}^*$$
$$\text{S2}': \mathbf{O_2} + 2^* \longleftrightarrow 2\text{O}^*$$

A series of surface reaction steps occur, generating N_2, N_2O and CO_2:

$$\text{S3}: \text{NO}^* + {}^* \longleftrightarrow \text{N}^* + \text{O}^*$$
$$\text{S4}: \text{NO}^* + \text{N}^* \longleftrightarrow \mathbf{N_2} + \text{O}^* + {}^*$$
$$\text{S5}: \text{NO}^* + \text{N}^* \longleftrightarrow \mathbf{N_2O} + 2^*$$
$$\text{S6}: \text{CO}^* + \text{NO}^* \rightarrow \mathbf{CO_2} + \text{N}^* + {}^*$$
$$\text{S7}: 2\text{N}^* \rightarrow \mathbf{N_2} + 2^*$$
$$\text{S8}: \text{CO}^* + \text{O}^* \longleftrightarrow \mathbf{CO_2} + 2^*$$

The measured temporal trends of N_2O and CO_2 over a complete lean-rich cycle leads to some interesting observations, suggesting a more complex mechanism than one represented by steps S1–S8. For example, experiments that we describe later suggest participation by isocyanate intermediates. Based on the previous studies reported in the literature, the isocyanates form on the PGM sites and migrate over to the support/storage phase:

$$\text{S9}: \text{N}^* + \text{CO} \longleftrightarrow \text{NCO}^*$$
$$\text{S10}: \text{N}^* + \text{CO}^* \longleftrightarrow \text{NCO}^* + {}^*$$
$$\text{S10}': \text{NO}^* + \text{CO}^* \longleftrightarrow \text{NCO}^* + \text{O}^*$$
$$\text{S11}: \text{NCO}^* + \text{S} \longleftrightarrow \text{NCO} - \text{S} + {}^*$$

where S denotes a site on the support or storage function. The above sequence of steps captures the main features of the NO + CO + O_2 on Pt reaction system, including the competitive NO and CO adsorption, CO oxidation, NO reduction, and isocyanate formation. It should be noted that though the catalyst employed contains both Pt and Rh, we consider the role of the total precious metal content rather than the individual effect of Pt and Rh as this is beyond the scope of the current study. Moreover, the effect of Rh has been investigated by several research groups before and is expected to increase the WGS activity and also provides excellent NO bond scission activity when added to a Pt based catalyst [51, 52]. Rh is considered to be a better NO_x reduction catalyst than Pt at lower temperatures (<250 °C) [50].

Figure 3 shows the N_2O (a) and CO_2 (b) temporal profiles over two lean-rich cycles for a CO feed concentration

of 1 % (10,000 ppm) and temperature range of 150–300 °C. At low temperatures (150–200 °C) the cycle-averaged CO conversion is much higher than the NO_x conversion; CO_2 generation is significant (Fig. 3b) while that of N_2O is comparatively much smaller (Fig. 3a). Two peaks were observed in the CO_2 concentration at 150 and 200 °C, before and after the switch from the rich phase to the lean phase. In fact, more than half of the generated CO_2 appeared during the lean phase, and most of that CO_2 was formed during the first few seconds of the lean phase.

Several features of the data in Fig. 3 are consistent with a periodic process dominated by strongly bound CO on Pt and Rh. At low temperature a high fractional CO coverage of the precious metal sites inhibits the adsorption and reaction of NO, key sequential steps for NO reduction [47]. Under these conditions CO oxidation, comprising steps S2, S2′, and S8, is dominant because the high coverage of CO inhibits the adsorption of NO (S1). The resulting low coverage of NO* means that the rates of subsequent steps like NO* dissociation (S3) and reactions between NO* (S4) and N* (S5) are negligible. By the end of the rich phase the catalyst surface is occupied by CO which, upon the introduction of the lean phase containing excess O_2, is oxidized to CO_2. Thus, most of the CO conversion observed in this lower temperature range is due to the oxidation of adsorbed CO by O_2 rather than by the reduction of NO. The difference in the extent of CO + O_2 and CO + NO reactions is due in part to the much higher gas phase concentration of O_2(4 %) compared to NO(500 ppm). At higher temperatures (≥250 °C) the inhibition by CO is diminished due to its increased desorption rate. The resulting lower coverage of CO enables more NO to adsorb and react. This is evidenced by the large increase in N_2O production at 250 and 300 °C (Fig. 3a).

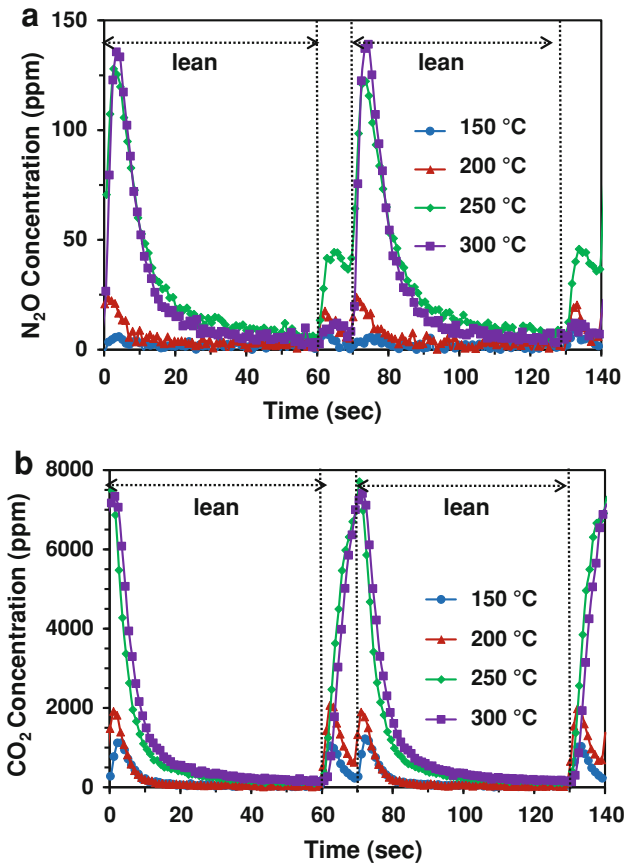

Fig. 3 Evolution of **a** N_2O and **b** CO_2 as a function of time during the reduction of NO_x by CO at 150, 200, 250 and 300 °C; each over two consecutive lean-rich cycles (*Lean* 500 ppm NO + 4 % O_2, 60 s; Rich: 1 % CO, 10 s; balance: Ar); Total flowrate: 3,000 sccm

It is well established in the literature that stable isocyanates (–NCO) are formed during the reduction of NO by CO on conventional Pt catalysts supported on oxides [20, 44]. Isocyanate formation proceeds through NO* dissociation (S3), followed by reaction of N* and CO* with reversible migration to the support (S); steps S9–S11. Previous studies have shown evidence for isocyanate participation during NSR on Pt/Ba catalysts like the Pt–Rh/Al_2O_3 catalyst used in the current study. The presence of a NO_x storage material (BaO) provides additional binding sites for the mobile isocyanates based on findings from in situ IR studies [40]. Nova and co-workers [31, 32, 40–43] suggested, based on reaction and surface IR measurements, that isocyanates are major intermediates during the reduction of NO_x by CO on NO_x storage catalysts and that the rate of isocyanate formation increases with CO concentration.

Other features of the temporal product data in Fig. 3, particularly those involving N_2O, suggest a more complex mechanism than the one described by steps S1–S8, one that involves an intermediate isocyanate species and function of the support/storage phase. Two N_2O peaks are noteworthy. The first N_2O peak obtained during the rich phase is likely due to the above-mentioned Pt-catalyzed reactions; viz. reaction step S5 and associated steps. The role of CO as surface oxygen scavenger (steps S6, S8) frees-up sites for spillover of NO_x species from the storage phase. It is the second N_2O peak observed during the lean phase that is of more interest and relevance to isocyanate participation. By the end of the rich phase the Pt crystallites has been exposed to an anaerobic, reducing environment. Isocyanate species are likely to have formed by reaction of CO with adspecies originating from the storage phase (N* and NO*; steps S9, S10, S10′). These isocyanates either accumulate on the Pt crystallites or migrate to the adjacent Al_2O_3 support and/or storage material BaO. Upon the start of the subsequent lean phase containing O_2, NO, and NO_2, reactions are initiated between these species and surface isocyanates, producing N_2, N_2O, and CO_2. These reactions result in a second peak in N_2O and CO_2. In fact, Fig. 3a

also shows that at the higher temperature of 300 °C almost no N_2O is formed during the rich phase while a large N_2O peak is observed during the first few seconds of the lean phase. A few research groups showed through catalyst surface infrared studies that the isocyanate formation increases with temperature in this range and reported a maximum in the NCO formation at ~300 °C [32, 34]. Our reactor data are consistent with those observations; upon increasing the temperature from 250 to 300 °C, the surface –NCO concentration increases which, as described in more detail below, favors N_2 formation during the rich phase. This helps to explain the drop in the N_2O peak during the rich phase compared to that at 250 °C. Indeed, Fig. 4 compares the evolution trends of N_2O at 250 and 300 °C for various CO feed concentrations during two consecutive lean rich cycles. It is seen that upon an increase in the CO concentration, the N_2O peak increases at both temperatures. This is also attributed to an increase in the surface concentration of isocyanate/cyanate species resulting from the increase in CO concentration.

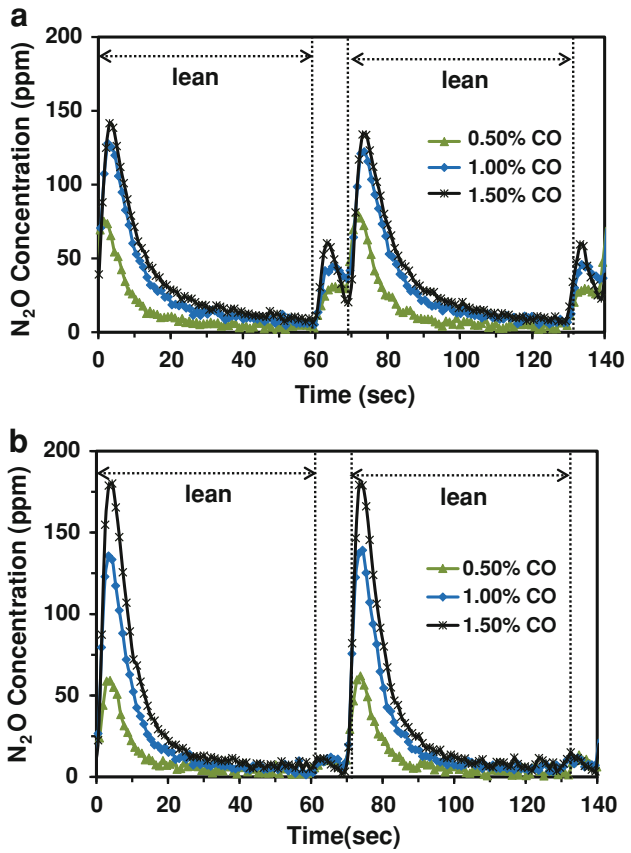

Fig. 4 Evolution of N_2O as a function of time during the reduction of NO by CO at **a** 250 °C and **b** 300 °C over two consecutive lean-rich cycles for different feed concentrations of CO during the rich phase (*Lean* 500 ppm NO + 4 % O_2, 60 s; Rich: 0.5, 1, 1.5 % CO, 10 s; balance: Ar); Total flowrate: 3,000 sccm

With the data now described and sets of various chemical reactions presented in the context of steps S1–S13, the overall mechanism on the PGM/Ba/Al catalyst is explained as follows. The reader is referred to Fig. 5. NO_x is stored in the form of nitrites [$Ba(NO_2)_2$] and nitrates [$Ba(NO_3)_2$] on the storage component during the lean phase [4, 8, 35, 41, 45, 46]. Additional reactions occur during this phase between gas phase species NO, O_2, and NO_2 and surface isocyanates formed during the previous regeneration phase. Some of the global reactions may include the following:

$$\mathrm{R1: Ba(NCO)_2 + 3/2\ O_2 \rightarrow N_2 + BaO + 2\mathbf{CO_2}}$$
$$\mathrm{R2: Ba(NCO)_2 + 2\ O_2 \rightarrow N_2O + BaO + 2\mathbf{CO_2}}$$
$$\mathrm{R3: Ba(NCO)_2 + 2\ NO + 3/2\ O_2 \rightarrow 2N_2O + BaO + 2\mathbf{CO_2}}$$
$$\mathrm{R4: Ba(NCO)_2 + 2NO + {}^1\!/_2O_2 \rightarrow 2N_2 + BaO + 2\mathbf{CO_2}}$$

The reactions are represented as gas-solid reactions, but it is likely that the NO and O_2 adsorb and react on the Pt crystallites. Kameoka et al. [27] studied the reaction of surface isocyanates with NO, O_2 and NO_2 on Ag/Al_2O_3 and Al_2O_3 catalyst and observed that while some N_2 formation was observed on just the Al_2O_3 support in the absence of Ag metal, the reactions appeared to be mostly Ag-catalyzed. Upon the switch to the rich phase, CO reduces the stored nitrates to surface intermediates like nitrites and isocyanate/cyanate species in addition to N_2 and N_2O [18, 34]. The reduction is thought to proceed catalytically through the reaction of CO* with NO_x species that spill over from the storage phase to the precious metal crystallites. It is convenient to represent the complex spillover and catalytic process by global reactions between CO and barium nitrate:

$$\mathrm{R5: Ba(NO_3)_2 + 4\mathbf{CO} \rightarrow \mathbf{N_2O} + BaCO_3 + 3\mathbf{CO_2}}$$
$$\mathrm{R6: Ba(NO_3)_2 + 5\mathbf{CO} \rightarrow \mathbf{N_2} + BaCO_3 + 4\mathbf{CO_2}}$$
$$\mathrm{R7: Ba(NO_3)_2 + 2\mathbf{CO} \rightarrow Ba(NO_2)_2 + 2\mathbf{CO_2}}$$
$$\mathrm{R8: Ba(NO_3)_2 + 8\mathbf{CO} \rightarrow Ba(NCO)_2 + 6\mathbf{CO_2}}$$

The barium isocyanate species so formed can further react with the other surface species like nitrates and nitrites to give N_2 and N_2O, as represented by the following reactions:

$$\mathrm{R9: Ba(NCO)_2 + Ba(NO_3)_2 \rightarrow 2\mathbf{N_2O} + 2BaCO_3}$$
$$\mathrm{R10: 5Ba(NCO)_2 + 3Ba(NO_3)_2 \rightarrow 8\mathbf{N_2} + 8BaCO_3 + 2\mathbf{CO_2}}$$
$$\mathrm{R11: Ba(NCO)_2 + 2\ Ba(NO_2)_2 \rightarrow 3\mathbf{N_2O} + 2BaCO_3 + BaO}$$
$$\mathrm{R12: Ba(NCO)_2 + Ba(NO_2)_2 \rightarrow 2\mathbf{N_2} + 2BaCO_3}$$

These global reactions lump together a myriad of surface steps, including nitrite/nitrate decomposition, NO/NO_2 spillover from the storage material to the Pt crystallites, and Pt-catalyzed reactions. An inspection of the stoichiometries for reactions R9 and R10 indicates that the ratio of surface

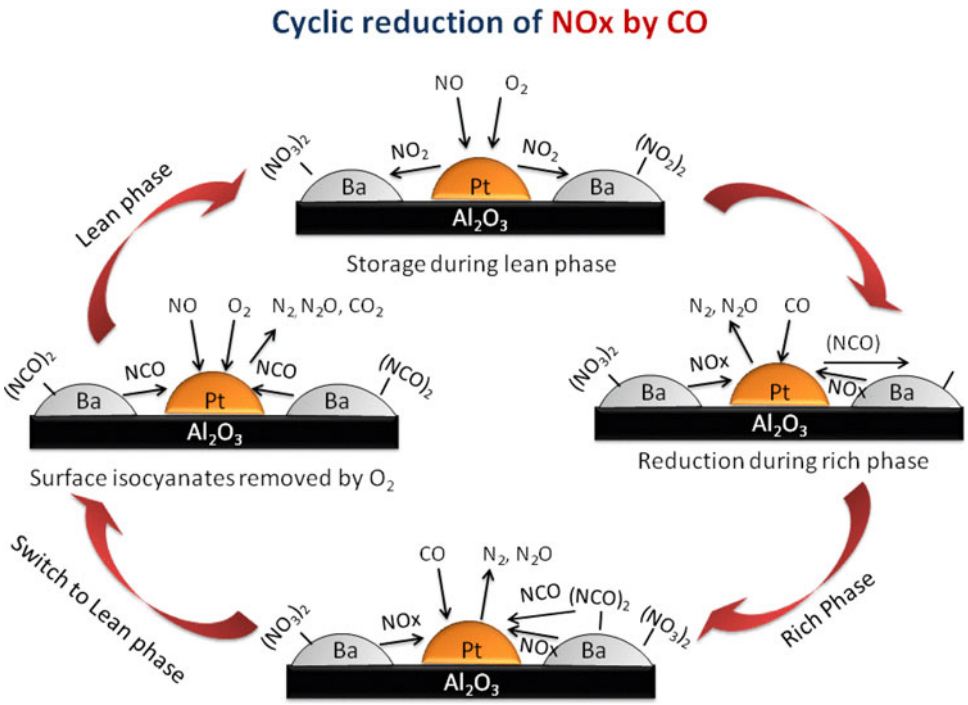

Fig. 5 Schematic representation of the proposed cyclic mechanism for the CO + NO

isocyanates/barium nitrate for N_2O formation is 1 while for N_2 formation is 1.67. Thus, a higher surface concentration of isocyanate favors N_2 formation. A similar observation can be made for the formation of N_2 and N_2O from reaction between isocyanates and nitrites; i.e., a higher surface isocyanate concentration favors N_2 formation over N_2O formation [stoichiometric ratio of isocyanates/nitrites is 1 for N_2 (R12) and 0.5 for N_2O (R11)].

An alternative, non-isocyanate mechanism leading to the evolution of second peak in N_2O during the lean phase involving the direct catalytic reduction of NO_x by adsorbed CO can be ruled out with targeted experiments. We carried out a steady-state experiment in which a mixture containing CO, NO, and O_2 with respective concentrations of 10,000, 500 ppm, and 5 % was fed over the same Pt–Rh/Al_2O_3 catalyst at 250 °C. Negligible conversion of NO (<5 %) was observed although complete conversion of CO was observed. This suggested that conventional Pt-catalyzed chemistry involving adsorbed NO and CO is negligible under lean conditions. This result gives more credence to reactions involving adsorbed isocyanates during the lean storage step when N_2O and CO_2 are evolved.

A revealing experiment that helps to confirm a role of isocyanates is to set up the conditions that synthesize surface NCO species, following procedures similar to the aforementioned spectroscopic studies [31, 32], and then to follow with different types of reacting species. This was done by subjecting the catalyst to sustained lean-rich switching at 250 °C involving a lean feed [NO(500 ppm)/O_2(5.0 %)/Ar] and a rich feed [CO(1.5 %)/Ar] until a transient steady state is reached. Then, at the end of the final rich phase, the catalyst was exposed to several different feeds: Pure Ar; NO(500 ppm) in Ar; O_2(4 %) in Ar; and NO(500 ppm) + O_2(4 %) in Ar. Fig. 6 compares the evolution of CO_2 (6a) and N_2O (6b) immediately upon the switch to the different feed gases. When exposed only to the inert carrier Ar, the catalyst released CO_2. A much smaller amount of N_2O was released after a 5 s delay. Similar evolution profiles were obtained with the three other feed gases, the one difference being the yields of CO_2 and N_2O were higher. These data are consistent with two reaction pathways. The release of CO_2 in an inert atmosphere is evidence for the thermal decomposition of $BaCO_3$:

$$\text{R13}: BaCO_3 \longleftrightarrow BaO + \mathbf{CO_2}$$

The delayed evolution of N_2O may suggest the decomposition of surface isocyanates by a decomposition and spillover process. The addition of O_2, NO, or NO/O_2 leads to a larger but nearly identical amount of CO_2 evolved with some differences in the evolution of N_2O. These data suggest the accumulation of NCO* and NCO–S species which decompose and/or react at elevated temperatures. The magnitude of CO_2 evolved cannot be explained by the accumulation of NCO on the Pt crystallites alone and could be a combination of $BaCO_3$ decomposition, NCO reaction with lean phase gases and also the oxidation of CO adsorbed on the catalyst surface at the end of the rich phase. Differences in the evolved N_2O concentration indicate some involvement of NO, NO_2 reacting

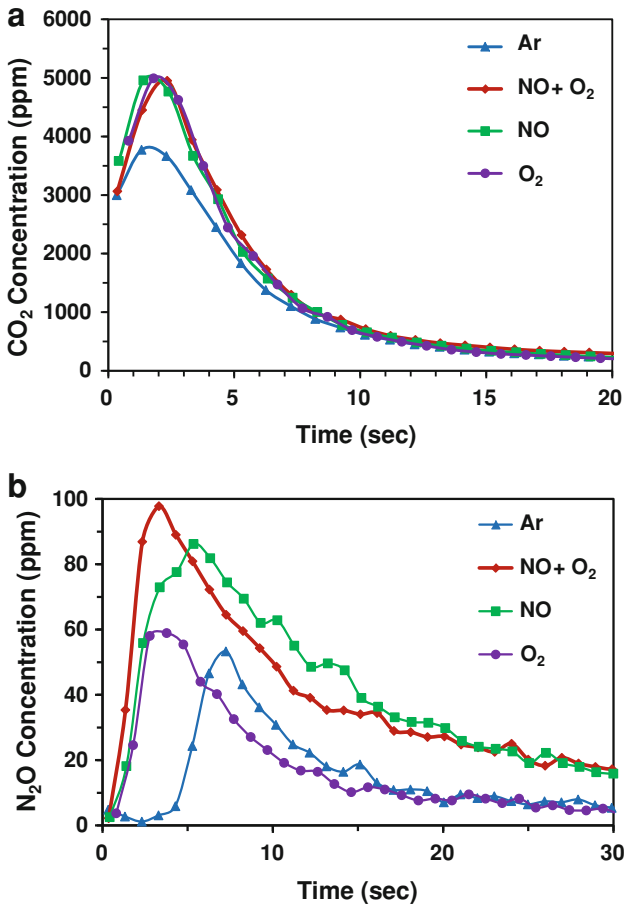

Fig. 6 Evolution of **a** CO_2 and **b** N_2O as a function of time upon the switch to the lean phase with different oxidizing systems after reaching a periodic steady state during the cyclic reduction of NO by CO(1.5 %) at 250 °C

with NCO species. Nevertheless, it is clear that N_2O and CO_2 generation during the lean phase, which is sustained throughout the lean phase if the CO pulse concentration and temperature are sufficiently high (Figs. 4, 6), is evidence for an isocyanate pathway.

3.2 Cyclic Reduction of NO_x by CO in the Presence of Excess H_2O

The cyclic reduction of NO_x by CO experiments were repeated in the presence of 5 % water over the entire lean and rich cycle. Figure 7a reports the cycle-averaged NO_x conversion as a function of temperature for lean-rich switching using three different reductants; H_2, CO, and CO + H_2O. These experiments are intended to check if H_2O has a promotional effect, such as through the aforementioned WGS reaction or the hydrolysis of isocyanate pathway. The data show that the H_2/Ar reductant mixture gave the highest NO_x conversion over the entire temperature range (Fig. 7a) and that the generated NH_3 is a monotonic decreasing function of the temperature (Fig. 7c). These results agree with previous reports [34]. The lower bound NO_x conversion was obtained when the 1.5 % H_2 was replaced by 1.5 % CO. The light-off temperature of CO oxidation on Pt is about 200 °C at these concentrations, so it is not surprising that the sharp jump in the CO conversion occurs in this range. When 5 % H_2O was added to the 1.5 % CO/Ar feed a notable increase in the cycle average NO_x conversion was observed, especially at temperatures ≥250 °C.

At low temperatures (150–200 °C) the addition of water had only a negligible effect, indicating that the reactions were slow and likely inhibited by CO. At these conditions the rate of the WGS reaction is quite low and therefore the production of H_2 is negligible (Fig. 7b). Along the same lines, were isocyanates formed under these conditions, one would expect a notable increase in the NH_3 through hydrolysis and a subsequent increase in NO_x reduction, but this is not the case. Thus, strongly bound CO inhibits the formation of NCO by inhibiting NO adsorption. The main effect of water addition at these low temperatures is the reduction in the NO oxidation activity of the catalyst during the lean phase as indicated by a decrease in the amount of NO_2 evolved when compared to same in the absence of water at the same temperature (not shown here). The addition of water has a detrimental effect on the oxidation activity of the catalyst and hence the drop in NO_2 concentration [47]. Most of the CO converted is due to its reaction with O_2 as indicated by the CO conversion being appreciably higher than the NO_x conversion at low temperature. This is consistent with the earlier results without water (Fig. 2).

At higher temperatures (≥250 °C) a significant promotional effect of water was observed. Over the 250–400 °C range the NO_x conversion increased by about 15 % points when H_2O was added (Fig. 7a). The NO_x conversion approached that of the H_2-only reductant results. Fig. 8 shows the effect of the CO feed concentration on the NO_x conversion (8a), CO conversion (8b), and product selectivity (8c) both in the absence and presence of H_2O(5 %) in the feed at 250 and 300 °C. A promotional effect of H_2O was observed for CO concentrations ≥15,000 ppm (1.5 %). Interestingly, the NO_x conversion increase was accompanied by a slight decrease in CO conversion under these conditions. The product distribution trends (Fig. 8c) reveal that the addition of H_2O leads to NH_3 generation for CO concentrations above 1 %, with the NH_3 concentration increasing with CO concentration at the expense of the N_2 selectivity. We elaborate on each of these findings below.

Interestingly, the cycle averaged NH_3 selectivity exhibited a local maximum at an intermediate temperature (Fig. 7c). At low temperatures (<250 °C) the NO_x conversion is quite low (Fig. 7a) as is the NH_3 selectivity

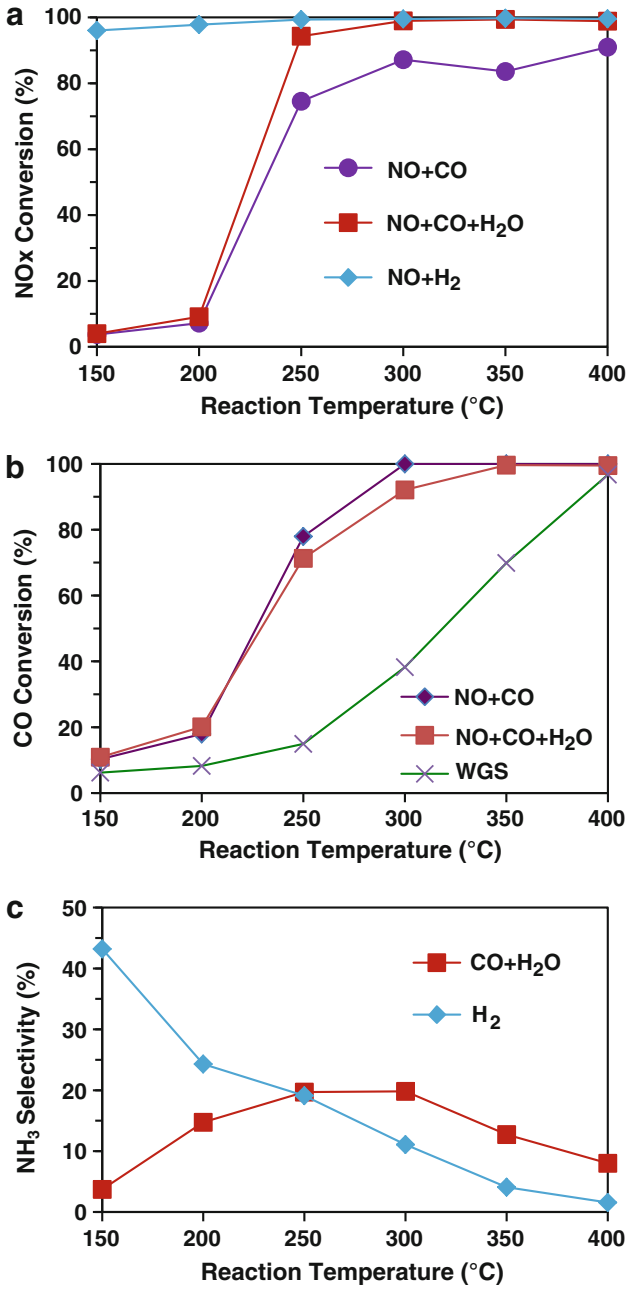

Fig. 7 Comparison of **a** Reactant NO_x conversion, **b** Reactant CO conversion and **c** Product selectivity to NH_3 during the reduction of NO_x by H_2 and by CO under dry conditions as well as in the presence of H_2O, as a function of the reaction temperature (*Lean* 500 ppm NO + 4 % O_2, 60 s; *Rich* 1.5 % CO or 1.5 % H_2 or 1.5 % CO + 5 % H_2O, 10 s; balance Ar); *Total flowrate* 3,000 sccm

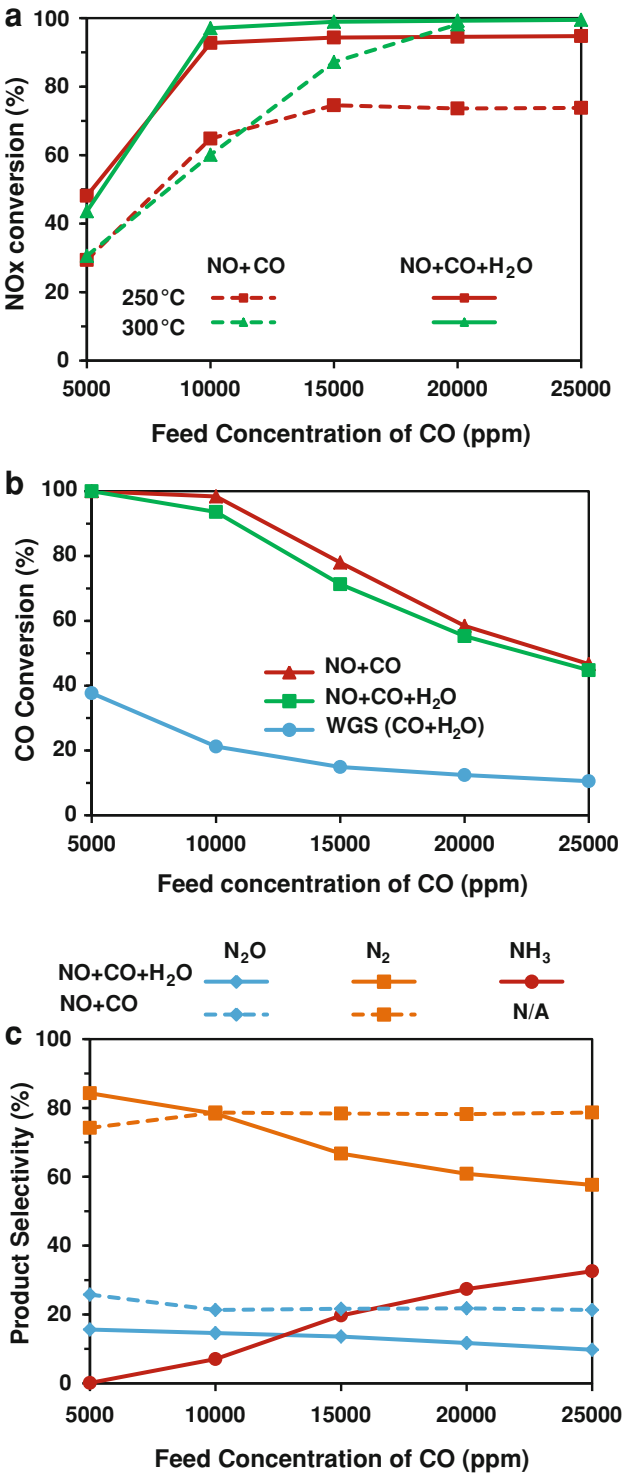

Fig. 8 Comparison of conversion of **a** NO_x at 250 and 300 °C and **b** CO at 250 °C during the reduction of NO_x by CO both in the presence and absence of excess water and also during the water gas shift reaction as a function of feed concentration of CO (*Lean* 500 ppm NO + 4 % O_2, 60 s; *Rich* 0.5–2.5 % CO, 10 s; *balance* 5 % H_2O: balance Ar). **c** Corresponding dependence of product selectivity to N_2, N_2O and NH_3 (*Lean* 500 ppm NO + 4 % O_2, 60 s; *Rich* 5,000–25,000 ppm of CO, 10 s; with and without 5 % H_2O: balance Ar)

(Fig. 7c). For reasons discussed earlier, strong adsorption by CO inhibits NSR. Moreover, the low WGS activity means that little H is available for NH_3 formation. Similarly, CO inhibits NCO formation. For temperatures above 250 °C the yield of NH_3 is higher for the CO + H_2O feed

than the H_2 feed. This counterintuitive result can be explained by differences in the spatial dependence of NH_3 production being different in the two cases. Previous spatiotemporal studies with H_2 as the reductant have shown that NH_3 formation occurs in the upstream section of the reactor. In its role as a H carrier, the NH_3 travels downstream and reacts with stored NO_x. This reduces the NH_3 selectivity and yield. In contrast, with CO + H_2O as the reductant feed, NH_3 generation is more spatially protracted because of the additional chemistry involved in generating H_2 and/or isocyanates during the rich pulse. As a result, NH_3 so formed encounters a shorter zone containing stored NO_x species. This explanation requires experiments that probe the spatial profile of NH_3 and are currently under investigation in our lab.

The enhancement in the NO_x conversion as a result of the H_2O addition is attributed to either of two mechanisms. As described earlier, the first mechanism is the formation of the more efficient NO_x reductant H_2 via the WGS reaction. The second mechanism is the hydrolysis of the intermediate isocyanate species by the excess water, leading to the enhanced regeneration of the storage sites.

The WGS mechanism is highlighted as follows (details as related to the steady state were described in [19]). Surface hydrogen produced by a combination of steps involving surface H_2O and CO, through a COOH* intermediate [48], leading ultimately to NH_3, as follows:

$$\mathrm{S12}: H_2O + {}^* \longleftrightarrow H_2O^*$$
$$\mathrm{S13}: H_2O^* + {}^* \longleftrightarrow OH^* + H^*$$
$$\mathrm{S14}: CO^* + OH^* \rightarrow COOH^* + {}^*$$
$$\mathrm{S15}: COOH^* \rightarrow CO_2 + H^*$$
$$\mathrm{S16}: 2\,H^* \longleftrightarrow H_2 + 2^*$$
$$\mathrm{S17}: H^* + NO^* \rightarrow HNO^* + {}^*$$
$$\mathrm{S18}: HNO^* + {}^* \rightarrow NH^* + O^*$$
$$\mathrm{S19}: HNO^* + {}^* \rightarrow N^* + OH^*$$
$$\mathrm{S20}: NH^* + H^* \rightarrow NH_2{}^* + {}^*$$
$$\mathrm{S21}: NH_2{}^* + H^* \rightarrow NH_3{}^* + {}^*$$
$$\mathrm{S22}: NH_3{}^* \longleftrightarrow NH_3 + {}^*$$

Thus, in addition to the direct reduction of NO_x by CO (steps S1–S11), the WGS mechanism involves the generation of H* adatoms that participate in the reduction of NO* supplied by the stored NO_x species through a spillover process.

On the other hand, the isocyanate hydrolysis involves the generation of NCO* species by reaction of CO* with N* or NO* (steps S9, S10, S10′), which migrate to the support and/or storage phase (step S11) and are hydrolyzed to NH_3. Global reactions that occur are as follows:

$$\mathrm{R14}: Ba(NCO)_2 + 3H_2O \rightarrow 2NH_3 + BaO + 2CO_2$$
$$\mathrm{R15}: Ba(NCO)_2 + 4H_2O \rightarrow 2NH_3 + Ba(OH)_2 + 2CO_2$$
$$\mathrm{R16}: 3Ba(NO_3)_2 + 10NH_3 \rightarrow 8N_2 + 3Ba(OH)_2 + 12H_2O$$
$$\mathrm{R17}: Ba(NO_3)_2 + 2NH_3 \rightarrow 2N_2O + Ba(OH)_2 + 2H_2O$$

It may also be speculated that the addition of water could eliminate the formation of spectator isocyanates observed by Burch and co-workers [38, 39] as the isocyanates are instantaneously hydrolyzed to NH_3, thereby preventing their buildup on the catalyst while preserving the NO_x storage capacity of the catalyst.

A comparison of the temporal product evolution trends in the presence and absence of water provides compelling evidence for the isocyanate hydrolysis mechanism. Figure 9 compares the temporal evolution of N_2O during the reduction of NO_x by CO both under dry and wet conditions at 250 °C. Under otherwise identical conditions, most of the N_2O is generated during the rich phase in the presence of water whilst most of it is generated during the first few seconds of the lean phase in the absence of water. This trend is difficult to explain with coupled NO_x reduction by WGS generated H_2. One would expect that N_2O, formed by step S5, or by NH_3 reacting with O* downstream, would lead to N_2O primarily appearing during the rich phase. That has been the reported temporal behavior with H_2 as the reductant [49]. The N_2O peak features can be best explained by the involvement of surface isocyanates. During the dry reduction of NO by CO, the catalyst surface accumulates NCO species, some remaining on the metal crystallites with the remainder migrating to the Al_2O_3 support and/or the BaO storage function. During lean-rich switching, a periodic steady state is established in which active isocyanates are formed and consumed, while spectator isocyanates reach a steady level, presumably further removed from the metal crystallites. During the lean phase the active isocyanate species react with the NO_x/O_2 and/or nitrates/nitrites to give N_2, N_2O and CO_2, as we have shown earlier in the context of Fig. 6. In contrast, in the presence of water the isocyanates are readily hydrolyzed to NH_3 during the rich phase and the product NH_3 may react further with stored NO_x and surface oxygen, forming N_2 and N_2O. The hydrolysis completely consumes the NCO species by the end of the rich phase. As a result, negligible N_2O is detected during the first few seconds of the subsequent lean phase because of the dearth of isocyanates in the vicinity of the Pt crystallites.

The slight decrease in CO conversion that accompanies the increase in NO_x conversion upon the addition of H_2O provides further evidence that favors the isocyanate regeneration mechanism while diminishing the importance of the WGS route. At first glance one would expect the CO

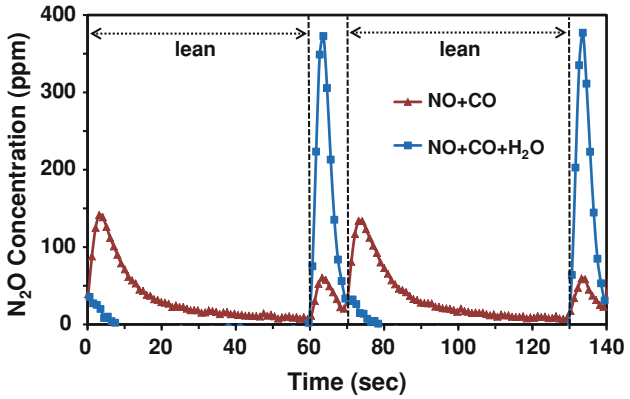

Fig. 9 Evolution of N_2O as a function of time during the reduction of NO by CO with and without water (5 %) at 250 °C over two consecutive lean-rich cycles (*Lean* 500 ppm NO + 4 % O_2, 60 s; Rich: 15,000 ppm of CO, 10 s; balance: Ar); Total flowrate: 3,000 sccm

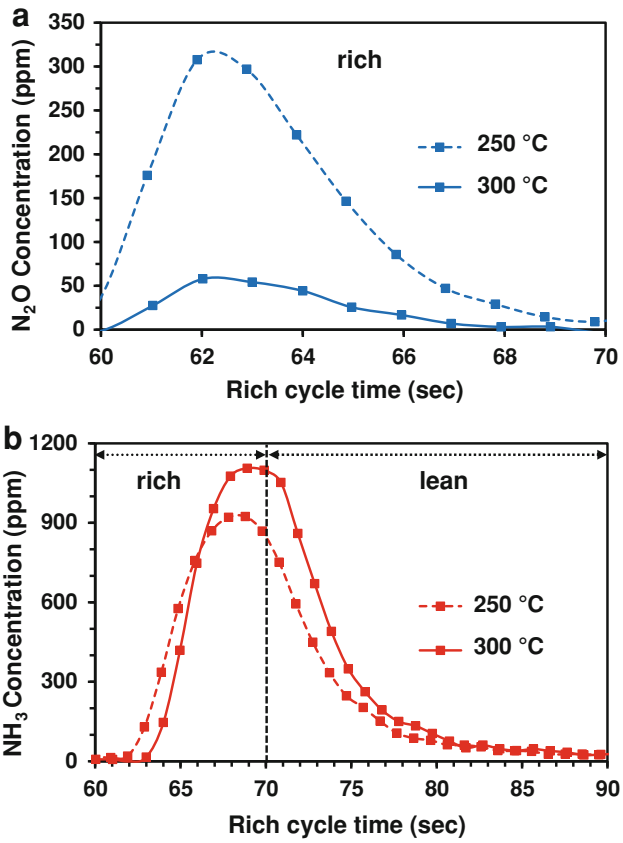

Fig. 10 Comparison of the evolution of **a** N_2O and **b** NH_3 during the reduction of NO_x by CO both in the presence of water (5 %) as a function of time during the rich phase at 250 and 300 °C (*Lean* 500 ppm NO + 4 % O_2, 60 s; *Rich* 2.5 % CO, 10 s; balance Ar); *Total flowrate* 3,000 sccm

conversion to increase if the NO_x conversion increases. Instead, the NO_x (CO) conversion increase (decrease) suggests a more efficient reductant utilization is achieved with the addition of water. Consider the following explanation. CO may reduce NO to N_2 or N_2O via the overall reactions

$$\text{R18 : NO} + \text{CO} \rightarrow 0.5\text{N}_2 + \text{CO}_2$$

$$\text{R19 : NO} + 0.5\text{CO} \rightarrow 0.5\text{N}_2\text{O} + 0.5\text{CO}_2$$

or may be oxidized by O_2 via

$$\text{R20 : CO} + 0.5\text{O}_2 \rightarrow \text{CO}_2$$

Now, for CO feed concentrations exceeding 3,000 ppm, CO is in stoichiometric excess: The lean $feed_f$ containing 500 ppm NO fed for 60 s requires a rich feed containing 3,000 ppm CO fed for 10 s to achieve the CO/NO = 1 required for NO reduction to N_2 (reaction R18). That the addition of H_2O results in an increase in NO_x conversion with a nearly constant or decreasing CO conversion means that the selectivity of lean NO_x reduction is more efficient. This is contrary to what would be encountered with a WGS mechanism, which requires that CO and H_2O be converted to CO_2 and H_2, and that the H_2 so generated is used to reduce NO. The NO and CO conversions in such a system should, in effect, be coupled. Figure 8b reports the CO conversion for the WGS reaction carried out periodically. There is a finite, nonzero CO conversion for all CO concentrations. Based on the above reasoning, one would expect that the CO conversion during NSR in the presence of water should increase by approximately the value of the WGS conversion when compared to the dry reduction of NO_x by CO. Instead, the CO conversion decreases. On the other hand, the isocyanate generation and hydrolysis pathway utilizes CO more efficiently through the sink-source function of the support/storage materials. NCO that is generated during the regeneration with CO may migrate to the support. In the absence of water a fraction of the NCO accumulates on the storage function and becomes spectators. In the presence of water the NCO species become reacting species due to their mobility and reactivity with H_2O. This enables CO to be more selectively utilized; i.e. the NCO that is formed serves as an intermediate for NH_3 and N_2 production, rather than a spectator in the absence of H_2O.

It should also be noted that the decrease in the CO conversion upon the addition of water is more pronounced at 300 °C than it is at 250 °C. This is consistent with the findings from Nova et al. [32, 34] who reported that the surface NCO formation is at a maximum at ~300 °C. Thus, the temperature increase from 250 to 300 °C should lead to increased generation of isocyanates, which in turn result in increased generation of NH_3 from the NCO hydrolysis. The NH_3 so formed can then regenerate additional stored NO_x. Thus, the enhanced CO utilization through isocyanate formation may be more significant at 300 °C.

The addition of water leads to a decrease in N_2O in the same temperature range, which suggests another benefit of

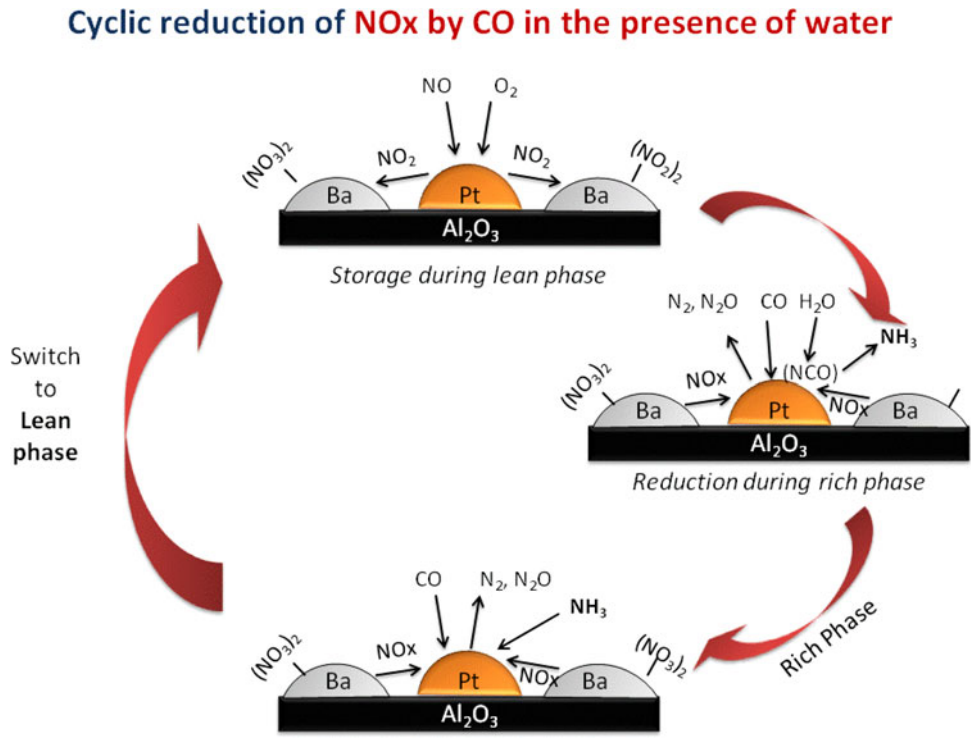

Fig. 11 Schematic representation of the proposed cyclic mechanism for the CO + NO + H_2O

the isocyanate mechanism. Figure 10 compares the evolution of N_2O and NH_3 during a rich phase (60–70 s) using CO as the reductant in the presence of excess water at 250 and 300 °C. The data show that the N_2O yield decreases sharply as the temperature increases. This may be explained by the enhanced formation of NH_3 from the hydrolysis of isocyanates which increases the ratio of NH_3/NO_x during the rich phase. A higher NH_3/NO_x stoichiometrically favors the formation of N_2 rather than N_2O as given by the following reactions:

$$\text{R21}: 3Ba(NO_3)_2 + 10NH_3 \rightarrow 8N_2 + 3Ba(OH)_2 + 12H_2O$$

$$\text{R22}: 3Ba(NO_3)_2 + 10NH_3 \rightarrow 8N_2 + 3BaO + 15H_2O$$

$$\text{R23}: Ba(NO_3)_2 + 2NH_3 \rightarrow 2N_2O + Ba(OH)_2 + 2H_2O$$

$$\text{R24}: Ba(NO_3)_2 + 2NH_3 \rightarrow 2N_2O + BaO + 3H_2O$$

Thus, the selectivity to N_2O drops and also the amount of NH_3 detected towards the end of the rich phase increases with the rise in temperature.

The mechanism of NO_x reduction by CO in the presence of water is shown in the schematic of Fig. 11. In the presence of water the isocyanates are readily hydrolyzed to NH_3 and hence no surface species are carried over from the rich phase after switching to the lean phase. The NH_3 also reduces the stored NO_x giving a deeper regeneration and enhances the NO_x reduction. These experimental results suggest that the surface NCO species are important reaction intermediates at moderate to higher temperatures (>200 °C) during the cyclic reduction of NO_x by CO.

4 Conclusions

During NSR on Pt–Rh/BaO/Al_2O_3, NH_3 may be generated by two major routes, the WGS route, in which NH_3 is generated by the catalytic reduction of NO by H_2 produced from the WGS reaction, and the isocyanate hydrolysis route, in which NH_3 is generated by the hydrolysis of surface isocyanates that are formed by the catalytic reaction of NO and CO. We have carried out a systematic study of the cyclic lean storage and reduction in the presence and absence of excess water to elucidate the NO_x and CO conversion and integral selectivity trends with particular focus on the NH_3 formation mechanism. New insight has been gained about the role of intermediate isocyanate species during the cyclic reduction of NO_x by CO. Under the transient aerobic conditions created by the lean-rich cycling, the generation, storage, supply, and reaction of isocyanates emerges as an important route guiding the NO_x reduction.

The transient reactor experiments support a mechanism in which isocyanates (–NCO) are formed during the reaction of NO and CO on the precious metal (PGM) and spill over to the neighboring Ba and Al sites. The isocyanates so formed further reduce the other stored NO_x to N_2 and N_2O depending on the surface concentration of isocyanates and nitrates/nitrites through precious metal catalyzed reactions. In the absence of water the catalyst is not completely regenerated during the rich phase and the catalyst surface still has surface isocyanates at the end of the rich phase. Moreover, spectator

isocyanates may migrate from the PGM-support interface, which may poison the NO_x storage capacity of the catalyst. The active isocyanates close to PGM-support interface react with NO and/or O_2 upon the switch to the lean phase and form N_2, N_2O and CO_2. As a result, NO_x is reduced both during the rich phase and also during the first few seconds of the successive lean phase. Higher surface concentration of isocyanates favors N_2 formation over N_2O.

On the addition of water to the NO–CO transient reduction system, isocyanates are readily hydrolyzed to NH_3 and CO_2 during the rich phase and the NH_3 further reduce the stored NO_x. Water also eliminates the buildup of spectator isocyanates on the catalyst surface and leads to the more efficient utilization of the reductant CO while preserving the storage capacity of the catalyst. As a result, the catalyst is deeply regenerated during the rich phase giving an enhancement in NO_x conversion with negligible net product evolution observed during the subsequent lean phase.

In summary, this study provides new data and insight about the cyclic storage and reduction of NO_x with CO as the reductant. The data reported here support the recent literature that isocyanates are important intermediate species and that the role of water enhances the utilization of the CO. Spatiotemporal studies are currently underway in our laboratory to build on the findings here to identify the best routes to N_2 by lean NO_x reduction.

Acknowledgments This research was supported by grants from the Texas Commission on Environmental Quality (TCEQ) and the Department of Energy Office of Vehicle Technologies (DE-EE0000205). We also acknowledge the catalyst division of BASF (Iselin, NJ) for providing the catalysts used in this study.

References

1. Ozkan US, Cai YP, Kumthekar MW, Zhang LP (1993) J Catal 142:182–197
2. Ozkan US, Cai YP, Kumthekar MW (1994) J Catal 149:390–403
3. Takahashi N, Shinjoh H, Lijima T, Suzuki T, Yamazaki K, Yokota K (1996) Catal Today 27:63–69
4. Epling WS, Campbell LE, Yezerets A, Currier NW, Parks JE (2004) Catal Rev Sci Eng 46:163–245
5. Hodjati S, Petit C, Pitchon V, Kiennemann A (2000) Appl Catal B 27:117–126
6. Schmitz PJ, Baird RJ (2002) J Phys Chem B 106:4172–4180
7. Cant NW, Patterson MJ (2002) Catal Today 73:271–278
8. Fridell E, Skoglundh M, Westerberg B, Johansson S, Smedler G (1999) J Catal 183:196–209
9. Nova I, Castoldi L, Lietti L, Tronconi E, Forzatti P, Prinetto F (2004) J Catal 222:377–388
10. Nova I, Lietti L, Castoldi L, Tronconi E, Forzatti P (2006) J Catal 239:244–254
11. Lietti L, Nova I, Forzatti P (2008) J Catal 257:270–282
12. Nova I, Lietti L, Forzatti P (2008) Catal Today 136:128–135
13. Cumaranatunge L, Mulla SS, Yezerets A, Currier NW, Delgass WN, Ribeiro FH (2007) J Catal 246:29–34
14. Harold MP (2012) Curr Opin Chem Eng 1:303–311
15. Mulla SS, Chaugule SS, Yezerets A, Currier NW, Delgass WN, Ribeiro FH (2008) Catal Today 136:136–145
16. Poulston S, Rajaram RR (2003) Catal Today 81:603–610
17. Liu ZQ, Anderson JA (2004) J Catal 228:243–253
18. Abdulhamid H, Fridell E, Skoglundh M (2004) Top Catal 30(1):161–168
19. Dasari PR, Muncrief R, Harold MP (2012) Catal Today 184:43–53
20. Unland ML (1973) J Phys Chem 77:1952–1956
21. Rasko J, Solymosi F (1980) J Chem Soc Farad Trans I(76):2383–2395
22. Rasko J, Solymosi F (1981) J Catal 71:219–222
23. Solymosi F, Sarkany J, Schauer A (1977) J Catal 46:297–307
24. Solymosi F, Volgyesi L, Sarkany J (1978) J Catal 54:336–344
25. Solymosi F, Rasko J (1980) J Catal 63:217–225
26. Hecker WC, Bell AT (1984) Appl Catal 85:389–397
27. Kameoka S, Chafik T, Ukisu Y, Miyadera T (1998) Catal Lett 55:211–215
28. Ukisu Y, Miyadera T, Abe A, Yoshida K (1996) Catal Lett 39:265–267
29. Solymosi F, Rasko J (1980) J Catal 10:19–25
30. Miners JH, Bradshaw AM, Gardner P (1999) Phys Chem Chem Phys 1:4909–4912
31. Forzatti P, Lietti L, Nova I, Morandi S, Prinetto F, Ghiotti G (2010) J Catal 274:163–175
32. Nova I, Forzatti P, Prinetto F, Ghiotti G (2010) Catal Today 151:330–337
33. Unland ML (1973) Science 179:567–569
34. Szailer T, Kwak JH, Kim DH, Hanson JC, Peden CHF, Szanyi J (2006) J Catal 239:51–64
35. Lesage T, Verrier C, Bazin P, Saussey J, Daturi M (2003) Phys Chem Chem Phy 5:4435–4440
36. Bion N, Saussey J, Haneda M, Daturi M (2003) J Catal 217:47–58
37. Scholz CML, Maes BHW, De Croon M, Schouten JC (2007) Appl Catal A 332:1–7
38. Chansai S, Burch R, Hardacre C, Breen J, Meunier F (2010) J Catal 276:49–55
39. Chansai S, Burch R, Hardacre C, Breen J, Meunier F (2011) J Catal 281:98–105
40. Nova I, Lietti L, Forzatti P, Frola F, Prinetto F, Ghiotti G (2009) Top Catal 52:1757–1761
41. Castoldi L, Lietti L, Forzatti P, Morandi S, Ghiotti G, Vindigni F (2010) J Catal 276:335–350
42. Castoldi L, Lietti L, Bonzi R, Artioli N, Forzatti P, Morandi S (2011) J Phys Chem C 115:1277–1286
43. Morandi S, Ghiotti G, Castoldi L, Lietti L, Nova I, Forzatti P (2011) Catal Today 176:399–403
44. Unland ML (1973) J Catal 31:459–465
45. Kabin KS, Khanna P, Muncrief RL, Medhekar V, Harold MP (2006) Catal Today 114:72–85
46. Muncrief RL, Khanna P, Kabin KS, Harold MP (2004) Catal Today 98:393–402
47. Toops TJ, Smith DB, Epling WS, Parks JE, Partridge WP (2005) Appl Catal B 58:255–264
48. Chen Y, Wang HF, Burch R, Hardacre C, Hu P (2011) Faraday Disc 152:121–133
49. Clayton RD, Harold MP, Balakotaiah V (2009) AIChE J 55:687–700
50. Yongjie R, Harold MP (2011) ACS Catal 1:969–988
51. Theis J, Ura J, McCabe RW (2007) SAE Trans 2007-01-1055
52. Gandhi HS, Graham GW, McCabe RW (2003) J Catal 216:433–442